

Sequential resonant tunneling of holes in GaAs-AlAs superlattices

Harald Schneider, Holger T. Grahn, Klaus v. Klitzing, and Klaus Ploog

Max Planck Institut für Festkörperforschung, Heisenbergstrasse 1, D-7000 Stuttgart 80, Federal Republic of Germany

(Received 22 May 1989)

We have studied carrier transport in an electric field perpendicular to the layers of GaAs-AlAs superlattices. We observed structures in the field dependence of the transport characteristics which are attributed to sequential-resonant-tunneling processes between hole subbands. This interpretation is strongly supported by the energy splitting between the valence subbands determined from photocurrent spectra. In addition, there is some experimental evidence that these transport processes take place not only between different heavy-hole subbands but also from heavy-hole subbands into light-hole subbands. The occurrence of the latter transport process is a direct consequence of the coupling between the light- and heavy-hole subbands at finite parallel momentum due to nonparabolicities.

Tunneling processes of holes through semiconductor barriers have recently been the subject of increasing theoretical interest¹⁻³ because of the complicated structure of the valence band of most III-V semiconductor materials. There are, however, only very few experimental results on hole tunneling published in the literature, e.g., resonant tunneling of holes in GaAs-AlAs double-barrier structures by Mendez *et al.*,⁴ while tunneling of electrons has been investigated extensively.⁵ Nevertheless, transport properties of holes are very important, especially for superlattices (SL's) in *p-i-n* diode photoconductors, since the space-charge properties of these systems are strongly influenced by transport processes. Due to the absence of positive space charge in such a structure, it was even suggested that heavy holes can tunnel across the barrier resonantly via deep impurity levels.⁶

In this paper we will present experimental results on sequential resonant tunneling between hole subbands. This type of transport processes can occur not only between subbands of the same kind of holes [heavy holes (hh), light holes (lh)] but also between hh and lh subbands. The latter phenomenon is explained by nonparabolicities of the valence subbands and has recently been treated theoretically.^{1,3} The energy spacings between the participating subbands can be determined by photocurrent spectroscopy.

We used in our measurements a SL consisting of 90 periods of nominally 5-nm GaAs and 2.2-nm AlAs. The SL is sandwiched between layers of 30-nm GaAs followed by 500-nm-wide Al_{0.5}Ga_{0.5}As window layers. The Al_{0.5}Ga_{0.5}As layers are *n*-doped at the substrate side and *p*-doped at the top side, both to about 10^{18} cm⁻³. The structure was grown by molecular-beam epitaxy on a (100)-oriented *n*⁺-type GaAs substrate and processed into mesas of 130 and 450 μ m diameter which were used for the transport and spectroscopic experiments, respectively. Ohmic contacts were provided by evaporation of Cr/Au (top side) and AuGe/Ni (substrate side).

For our transport experiments, we used a 670-nm laser diode (Toshiba) driven by a fast-pulse generator (Avtech) at 1 MHz repetition rate. The laser provided light pulses of 80 ps duration which were focused onto the sample. In this way, both electrons and holes were injected into the

SL. At first sight, one would assume that the electrons should move much faster than the holes because of the different effective masses. However, it will be shown later that transport by hole tunneling can actually occur faster than transport by electron tunneling, provided that the valence subbands are at resonance and that the conduction subbands are off resonance.

In Fig. 1, we have plotted static current-voltage curves which were obtained with a picoampere meter. Under reverse bias (negative sign of the applied voltage), the photocurrent saturates at 90 nA for high electric fields. Assuming a quantum efficiency of 1 and complete relaxation of the system between the light pulses, this saturation level corresponds to an injected carrier density of about 3×10^{14} cm⁻³ per light pulse which is well below the estimated residual doping ($\approx 10^{15}$ cm⁻³). The increase close to -20 V is due to the onset of avalanche multiplication. In forward bias, the current of the illuminated sample changes its sign at about 1.7 V. At this value the external electric

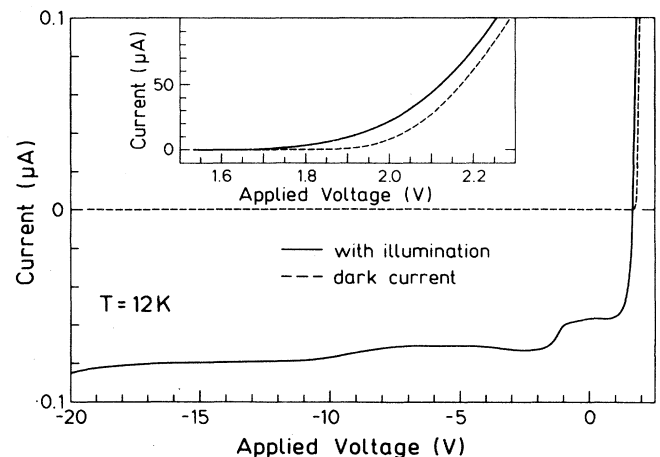


FIG. 1. Current-voltage characteristics at 12 K with and without illumination. The illumination conditions are described in the text. The inset shows the range of positive electric fields on an expanded scaled.

field compensates the built-in field so that the total electric field is zero. The sign reversal is followed by a sharp increase of the current, with and without illumination. This regime is shown in the inset. Note that the current under illumination now differs from the dark current by about $20 \mu\text{A}$. Such an effect ("effective-mass filtering") was previously observed by Capasso *et al.*⁷ in a $\text{Al}_{0.48}\text{In}_{0.52}\text{As-Ga}_{0.47}\text{In}_{0.53}\text{As}$ superlattice and will not be discussed further in this paper.

In the context of sequential resonant tunneling, the important feature shown in Fig. 1 manifests itself in the observed increase of the photocurrent which saturates close to the bias voltages of -2.2 and -11 V. Since the generation rate of photocarriers at 670 nm is approximately independent of the bias, this structure is caused by the competitive behavior between the transport and the recombination processes. When the drift velocity increases, less carriers have time to recombine and the efficiency for carrier collection at the contacts increases.

In contrast to the static photocurrent which reflects the temporal mean value of the signal, the amplitude of the transient photocurrent strongly depends on the *dynamical* behavior of the conduction processes. We therefore recorded the peak value of the photocurrent under pulsed illumination conditions as described above. In this experiment, the current was detected by a sampling oscilloscope (Tektronix) which had an analog interface. The illumination was mechanically chopped at 120 Hz and the signal of the analog output of the oscilloscope was recorded by a lock-in amplifier. This procedure provided a highly stable signal and a very efficient base line correction. The overall bandwidth was about 4 GHz.

The voltage dependence of the peak photocurrent is shown in Fig. 2. The local extremum at about 0.5 V is caused by the transition from minibandlike conduction processes at small electric fields to sequential tunneling between localized states at higher fields. The decrease of the absolute value of the peak photocurrent with increasing electric field (between 0.5 and -1 V) is directly related to a decrease of the drift velocity.^{8,9} At a temperature

of 12 K, a similar structure is also observed for total electric fields pointing in the opposite direction (at 2.0 – 2.5 V forward bias).

The local extremum at 0.5 V in Fig. 2 is followed by a peak at -2.2 V which is also associated with a negative differential dependence of the peak photocurrent (between -2.5 and -5 V) on the electric field. We note that this behavior is accompanied by an increase in the duration of the photocurrent transients (from about 1 ns at -2.2 V to 4 ns at -7 V). Another less pronounced structure is seen at -11 V.

The structure at a positive bias of 2 – 2.5 V is smeared out at higher temperatures since the dark current increases due to stronger carrier injection at the contacts. The other features, however, are equally well resolved at 80 K (see Fig. 2). Even at room temperature, the negative differential behavior of the peak photocurrent is maintained.

These features strongly suggest that resonant tunneling processes must be involved. We therefore determine the voltage drop across one superlattice period at the bias values where these structures appear. The electric field is calculated by dividing the applied plus built-in voltage by the total width w of the depletion zone. For this purpose, w is obtained from capacitance-voltage measurements. Due to a partial depletion of the contacts, w exceeds the total width of the superlattice, as determined from the growth parameters, by about 10% (at 0.5 and -2.2 V) and 15% (at -11 V). We obtain for our superlattice a voltage drop of 12 , 39 , and 120 mV per SL period at a bias of 0.5 , -2.2 , and -11 V, respectively.

The first value agrees reasonably well with the electric field that corresponds to the situation that the voltage drop per period equals the calculated width Δ of the lowest conduction miniband ($\Delta = 10$ meV). We therefore associate it with field-induced carrier localization.¹⁰ We note that a similar effect has been reported in Refs. 8 and 9. Of course, in the present context, it is not only related to electrons but it arises from the transition from minibandlike conduction to sequential nonresonant tunneling of *all* the carriers in the system.

In order to relate these transport data to the *actual* subband structure of our sample, it is now essential to determine the energy spacings between the subbands from an independent experiment. This is achieved by photocurrent spectroscopy.^{8,11} Spectra at three different bias voltages are shown in Fig. 3. As sketched in the inset, we clearly observe the heavy-hole excitons (hh1) and the light-hole excitons (lh1). Additionally, there is a third (forbidden) transition which only becomes visible at very high electric fields and is associated with the lowest conduction subband and the first excited heavy-hole subband (hh2). Except for excitonic corrections, the energy spacings between these transitions directly coincide with the intersubband energy of the valence band, i.e., 43 meV (between the hh1 and lh1 subbands) and 118 meV (between hh1 and hh2).

We have attempted to calculate these energy spacings. The Luttinger Hamiltonian, as used in Refs. 2 and 3, is a more accurate representation of the actual band structure than the usual one-band model. In practice, however, the problem consists of knowing the correct semiempirical

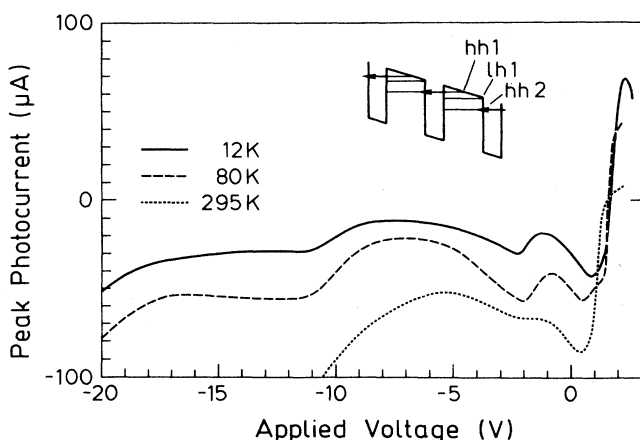


FIG. 2. Peak photocurrent vs applied voltage at different temperatures. The schematics of sequential resonant hole tunneling (corresponding to the situation at -11 V) is also shown.

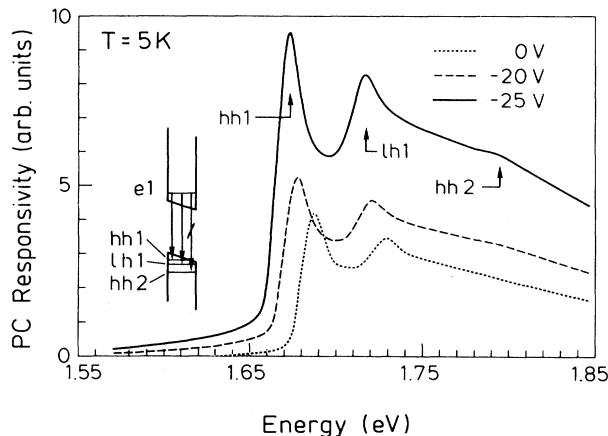


FIG. 3. Photocurrent (PC) responsivity (i.e., photocurrent corrected for the spectral dependence of the light source) vs energy at different bias. The increase of the signal for -20 and -25 V is due to avalanche multiplication. The observed transitions are sketched in the inset.

band parameters. The calculations in Refs. 2 and 3 were performed for essentially the same quantum well system and are based on effective-mass values between 0.45 and 0.6 free-electron masses m_0 for heavy holes in GaAs. The obtained intersubband energies range from 58 to 74 meV (between hh1 and hh2) and from 152 to 217 meV (between hh1 and hh3) which are far from the spacing between the hh1 exciton and the forbidden transition observed in the photocurrent spectra (Fig. 3). At the same time, a hh1-lh1 splitting of 63–78 meV (Ref. 2) and 45 meV (Ref. 3) was found.

A value of $0.34m_0$ for the hh effective mass in GaAs quantum wells was proposed by Miller *et al.*¹² in order to fit their experimental excitonic transition energies in GaAs-Al_{0.3}Ga_{0.7}As quantum wells. With this value we obtained a spacing of 86 meV between the hh1 and hh2 subbands using a one-band model. The difference between this value of the hh splitting and the experimentally observed one can have several origins. First, the actual well width can deviate from the nominal one. However, the observed energy position of the hh1 transition suggests that this deviation is less than 10% while we need at least 15% in order to get the experimental hh1-hh2 spacing. Second, there exists a large difference between the hh mass of bulk GaAs and the mass parameters adopted for wide quantum wells¹² which leads to uncertainties in the underlying band parameters.

Since the experimental subband spacings coincide well with the ones expected from our transport experiments, we conclude that the sequential resonant tunneling picture, as sketched in the inset of Fig. 2, is valid, i.e., that we have observed tunneling processes between different valence subbands. While resonant hh1 \rightarrow hh2 tunneling works in the same way as in the conduction band, resonant hh1 \rightarrow lh1 tunneling is a more complicated process. This transition was theoretically predicted in Refs. 1 and 3. In a multiband approach, it is forbidden at zero momentum

k_{\parallel} parallel to the layers of the superlattice. This selection rule becomes violated at finite k_{\parallel} due to the nonparabolicities of the valence bands. Apparently, the reason why it can be seen in our experiment is the fact that the corresponding tunneling probability is relatively large since lh-like subbands have much smaller effective masses than the hh-like ones.¹ Similar interaction phenomena between hh- and lh-like states have been previously observed to cause anticrossing phenomena between exciton energies.¹³

However, we should keep in mind that the observed lh-hh splitting lies between the LO-phonon energies of GaAs and AlAs. Inelastic LO-phonon assisted tunneling processes have been observed to produce extra peaks in the current-voltage characteristics of double barrier diodes¹⁴ and could eventually cause structures in the present SL at the same electric fields as expected for the case of resonant hh1 \rightarrow lh1 tunneling. But, from the fact that the structure at -2.2 V (Fig. 2) is very pronounced even at room temperature, it seems that hh1 \rightarrow lh1 tunneling is actually the dominating transport process.

It is interesting to discuss the dynamics of the observed photocurrent transients at the different bias voltages. Previously,^{8,9,15} we have studied the transit times for electron transport through GaAs-AlAs SL's with similar barrier thicknesses d_{AlAs} but with much wider wells ($d_{\text{GaAs}} = 12\text{--}14$ nm). It follows from those data that transport times of about 4 ns for nonresonant sequential tunneling across the present SL system seem realistic also for electrons. We note that the amplitude measurement as shown in Fig. 2 is particularly sensitive to the fastest component of the moving carriers. We did not find any indication, e.g., at a bias of -6 V, of faster carrier components although the experimental bandwidth was large enough. Therefore, we conclude that, for the SL studied here, transport due to sequential resonant tunneling from hh into lh as well as from hh into higher hh subbands occurs faster than transport due to nonresonant tunneling of electrons.

In summary, we have presented time-resolved photoconduction experiments which, together with our spectroscopic results, show that sequential resonant tunneling processes between different valence subbands dominate the photoconduction characteristics of undoped GaAs-AlAs SL's for certain parameters ($d_{\text{GaAs}} = 5$ nm, $d_{\text{AlAs}} = 2$ nm). We have observed these transport processes to occur between different hh subbands. We also found experimental evidence for tunneling processes from the lowest hh subband into the lowest lh subband. The latter process is eventually influenced by inelastic phonon-assisted tunneling since the energy splitting between these subbands is of the order of the LO-phonon energies. Resonant tunneling between hh and lh states can be explained within a multiband approach by the nonparabolicities of the valence bands.

The authors are grateful to M. Hauser for sample growth, to I. Jungbauer, F. Schartner, S. Tippmann, and M. Wurster for diode processing, and to J. Behring, M. Schmid, and G. Wilk for technical support. This work was partially supported by the Bundesministerium für Forschung und Technologie.

- ¹K. V. Rousseau, J. N. Schulman, and K. L. Wang, in *Quantum Well and Superlattice Physics II*, edited by F. Capasso, G. H. Döhler, and J. N. Schulman, SPIE Conference Proceedings No. 943 (International Society for Optical Engineering, Bellingham, WA, 1988), p. 30.
- ²J.-B. Xia, *Phys. Rev. B* **38**, 8365 (1989).
- ³R. Wessel and M. Altarelli, *Phys. Rev. B* **39**, 12802 (1989).
- ⁴E. E. Mendez, W. I. Wang, B. Ricco, and L. Esaki, *Appl. Phys. Lett.* **47**, 415 (1985).
- ⁵Reviews can be found in L. Esaki, *IEEE J. Quantum Electron.* **QE-22**, 1611 (1986); F. Capasso, K. Mohammed, and A. Y. Cho, *ibid.* **QE-22**, 1853 (1986).
- ⁶F. Capasso, K. Mohammed, and A. Y. Cho, *Phys. Rev. Lett.* **57**, 2303 (1986).
- ⁷F. Capasso, K. Mohammed, A. Y. Cho, R. Hull, and A. L. Hutchinson, *Appl. Phys. Lett.* **47**, 420 (1985); *Phys. Rev. Lett.* **55**, 1152 (1985).
- ⁸H. Schneider, K. v. Klitzing, and K. Ploog, *Superlattices Microstruct.* **5**, 383 (1989).
- ⁹H. Schneider, K. v. Klitzing, and K. Ploog, *Europhys. Lett.* **8**, 575 (1989).
- ¹⁰J. Bleuse, G. Bastard, and P. Voisin, *Phys. Rev. Lett.* **60**, 220 (1988); E. E. Mendez, F. Agulló-Rueda, and J. M. Hong, *Phys. Rev. Lett.* **60**, 2426 (1988).
- ¹¹R. T. Collins, K. v. Klitzing, and K. Ploog, *Phys. Rev. B* **33**, 4378 (1986).
- ¹²R. C. Miller, D. A. Kleinmann, and A. C. Gossard, *Phys. Rev. B* **29**, 7085 (1984).
- ¹³L. Viña, R. T. Collins, E. E. Mendez, and W. I. Wang, *Phys. Rev. Lett.* **58**, 832 (1987).
- ¹⁴V. J. Goldman, D. C. Tsui, and J. E. Cunningham, *Phys. Rev. B* **36**, 7635 (1987); M. L. Leadbeater *et al.*, *ibid.* **39**, 3438 (1989).
- ¹⁵H. Schneider, W. W. Rühle, K. v. Klitzing, and K. Ploog, *Appl. Phys. Lett.* **54**, 2656 (1989).